

Sharp Valence Change as Origin of Drastic Change of Fermi Surface and Transport Anomalies in CeRhIn₅ under Pressure

Shinji Watanabe, Kazumasa Miyake

Graduate School of Engineering Science, Osaka University, Toyonaka, Osaka 560-8531, Japan

Abstract. The drastic changes of Fermi surfaces as well as transport anomalies near $P = P_c \sim 2.35$ GPa in CeRhIn₅ are explained theoretically from the viewpoint of sharp valence change of Ce. It is pointed out that the key mechanism is the interplay of magnetic order and Ce-valence fluctuations. It is shown that the antiferromagnetic state with "small" Fermi surfaces changes to the paramagnetic state with "large" Fermi surfaces with huge enhancement of effective mass of electrons with keeping finite c-f hybridization. This naturally explains the de Haas-van Alphen measurement and also the transport anomalies of T -linear resistivity emerging simultaneously with the residual resistivity peak at $P = P_c$ in CeRhIn₅.

1. Introduction

A heavy electron metal CeRhIn₅ has attracted much attention recently since it has been recognized to offer a new insight into the quantum critical phenomena by accumulated experimental studies. By applying pressure under the magnetic field larger than the upper critical field, the antiferromagnetic (AF) order is suppressed abruptly at $P = P_c \approx 2.35$ GPa [2]. The de Haas-van Alphen (dHvA) measurement revealed that the Fermi surfaces (FS) change from approximately the same FS as those of LaRhIn₅ to FS similar to those of CeCoIn₅ at $P = P_c$ with huge mass enhancement toward $P = P_c$. Transport anomalies such as emergence of T -linear resistivity and enhancement of residual resistivity are prominent near $P = P_c$ [3, 4, 5]. So far, it has been considered that localized-to-itinerant transition of f electrons might explain these anomalies [4]. However, this scenario encounters a serious difficulty in elucidating the experimental fact that the Sommerfeld constant at ambient pressure $P = 0$ in CeRhIn₅, $\gamma = 50$ mJ/molK², is about 10-times larger than that of LaRhIn₅ [2], which strongly suggests that heavy quasiparticles are formed in the AF-ordered state, showing an importance of hybridization between f and conduction electrons.

In this paper, we propose a unified explanation for resolving this outstanding puzzle in CeRhIn₅. First, we point out that the emergence of T -linear resistivity and residual-resistivity peak are quite similar to the observations in CeCu₂Ge₂ [6], CeCu₂Si₂ [7], and CeCu₂(Si_xGe_{1-x})₂ [8] at pressure $P = P_v$ located at higher pressure side than the AF-paramagnetic boundary $P = P_c$. The Cu-NQR measurement detected that the electric-field gradient starts to change at $P = 4$ GPa slightly less than $P_v \approx 5$ GPa where Ce valence changes [9]. Theoretically, it has been shown that enhanced valence fluctuations cause the T -linear resistivity [7] and residual-resistivity peak at $P = P_v$ [10]. Since in CeRhIn₅ such a

transport anomalies occur at the pressure of the AF-paramagnetic boundary, P_c seems to almost coincide with P_v , i.e., $P_c \approx P_v$. Below we demonstrate theoretically that this situation is indeed realized for realistic parameters for CeRhIn₅ and show that the interplay of the AF order and Ce-valence fluctuations is a key mechanism for resolving the outstanding puzzle in CeRhIn₅ in a unified way [11].

2. Model Calculation and Results

Let us start our discussion by introducing a minimal model which describes the essential part of the physics of CeRhIn₅ in the standard notation:

$$\mathcal{H} = H_c + H_f + H_{\text{hyb}} + H_{U_{fc}}, \quad (1)$$

where $H_c = \sum_{\mathbf{k}\sigma} \varepsilon_{\mathbf{k}} c_{\mathbf{k}\sigma}^\dagger c_{\mathbf{k}\sigma}$ represents the conduction band, $H_f = \varepsilon_f \sum_{i\sigma} n_{i\sigma}^f + U \sum_{i=1}^N n_{i\uparrow}^f n_{i\downarrow}^f$ the f level ε_f and onsite Coulomb repulsion U for f electrons, $H_{\text{hyb}} = V \sum_{i\sigma} (f_{i\sigma}^\dagger c_{i\sigma} + c_{i\sigma}^\dagger f_{i\sigma})$ the hybridization V between f and conduction electrons, and $H_{U_{fc}} = U_{fc} \sum_{i=1}^N n_i^f n_i^c$ the Coulomb repulsion U_{fc} between f and conduction electrons. The $H_{U_{fc}}$ term is a key ingredient for explaining the various anomalies caused by enhanced Ce-valence fluctuations: The T -linear resistivity and residual resistivity peak have been shown theoretically on the basis of this model eq. (1) [7, 10]. To discuss CeRhIn₅, we analyze this model by taking into account existence of the AF order. To make a comparison with the dHvA measurement for the β_2 branch which is a two-dimensional-like cylindrical Fermi surface, we consider the AF order with the ordered vector $\mathbf{Q} = (\pi, \pi)$ on the square lattice with $\varepsilon_{\mathbf{k}} = -2t(\cos(k_x) + \cos(k_y))$ at the filling $n \equiv (\bar{n}_f + \bar{n}_c)/2 = 0.9$ with $\bar{n}_f \equiv \sum_{\mathbf{k}\sigma} \langle f_{\mathbf{k}\sigma}^\dagger f_{\mathbf{k}\sigma} \rangle / N$ and $\bar{n}_c \equiv \sum_{\mathbf{k}\sigma} \langle c_{\mathbf{k}\sigma}^\dagger c_{\mathbf{k}\sigma} \rangle / N$. We take $t = 1$ as an energy unit.

To treat the effects of the AF order and Ce-valence fluctuations on equal footing, we apply the slave-boson mean-field theory [12] to eq. (1) [11]. The resultant ground-state phase diagram is shown in Fig. 1(a). The first-order valence transition (solid line with triangles) terminates at the quantum critical end point (filled circle), i.e., the QCP, and the valence crossover occurs at the dashed line with open circles. At the QCP the valence fluctuation diverges and the enhanced valence fluctuations appear even far away from the QCP, as indicated by enhanced valence susceptibility $\chi_v \equiv -\partial \bar{n}_f / \partial \varepsilon_f$ in Fig. 1(b) calculated for moderate U_{fc} 's. These are the results obtained within the paramagnetic solutions. The result when the AF order is taken into account is shown as the solid line with filled squares in Fig. 1(a). One can see that the AF-paramagnetic boundary, which is the first-order transition, almost coincides with the first-order valence-transition line and the valence-crossover line. This result is favorably compared with the observations in CeRhIn₅. When pressure is applied to the Ce compounds, ε_f increases. Thus, ε_f can be regarded as pressure. As shown in Fig. 1(a), the AF order is suppressed at the Ce-valence transition and crossover points, which indicates that the suppression is caused by the valence transition or enhanced valence fluctuations. This result implies that $P_c \approx P_v$ observed in CeRhIn₅ is reproduced by our model eq. (1). For comparison, hereafter, we show our results for $U_{fc} = 0.5$, which is a moderate U_{fc} as expected to be a realistic parameter for CeRhIn₅.

Figures 2(a) and 2(b) show the contour plots of the lower hybridized band with minority spin for $\varepsilon_f = -0.29$ and $\varepsilon_f = -0.28$, respectively. Here, we apply the magnetic field to the system as $\mathcal{H} - h \sum_i (S_i^{fz} + S_i^{cz})$ with $h = 0.005$ to simulate the field of $H = 15$ T used in the dHvA measurement [2]. We have verified that the drastic change of the Fermi surface occurs at the AF-paramagnetic-transition point $\varepsilon_f = \varepsilon_f^c = -0.283$: Folded Fermi surface in Fig. 2(a) in the AF phase changes to the unfolded Fermi surface in Fig. 2(b) in the paramagnetic phase as ε_f passes across ε_f^c . We note here that the dashed line represents the Fermi surface of conduction electrons at $\bar{n}_c = 0.8$. This is the small Fermi surface obtained by setting $V = 0$ in the model eq.(1), where f electrons with $\bar{n}_f = 1$ are completely localized. One can see that the Fermi surface in the AF phase calculated for finite V is nearly the same as the “small” Fermi surface.

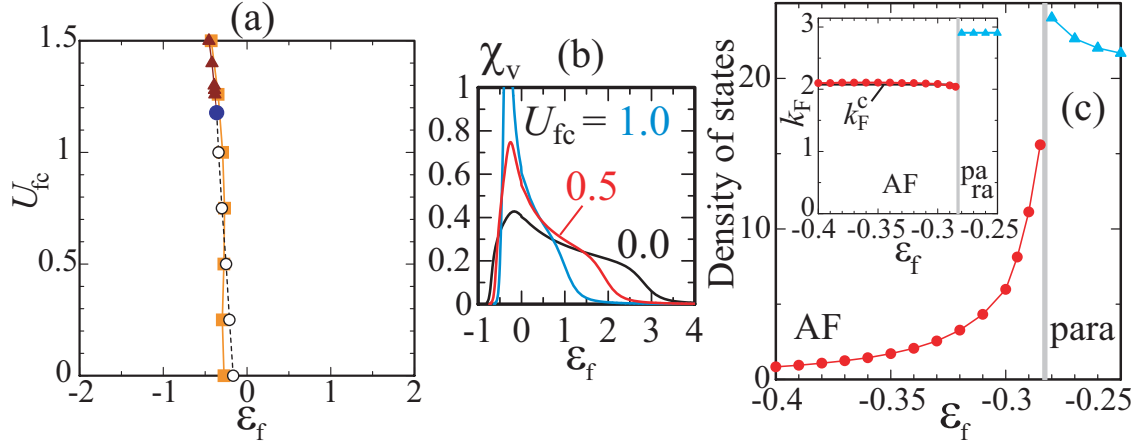


Figure 1. (color online) (a) Ground-state phase diagram in the U_{fc} - ϵ_f plane for paramagnetic and AF states (see text). The first-order valence-transition line (solid line with triangles) terminates at the quantum critical end point (filled circle). Valence crossover occurs at the dashed line with open circles, at which χ_v has a maximum, as shown in (b). The solid line with filled squares represents the boundary between the AF state and the paramagnetic state. (c) Total density of states vs ϵ_f for $U_{fc} = 0.5$. The inset shows k_F vs ϵ_f : In AF phase, black line represents the small Fermi surface of conduction electrons $\epsilon_{\mathbf{k}}$ at $\bar{n}_c = 0.8$. All results in (a)-(c) are calculated for $t = 1$, $V = 0.2$, and $U = \infty$ at $n = 0.9$.

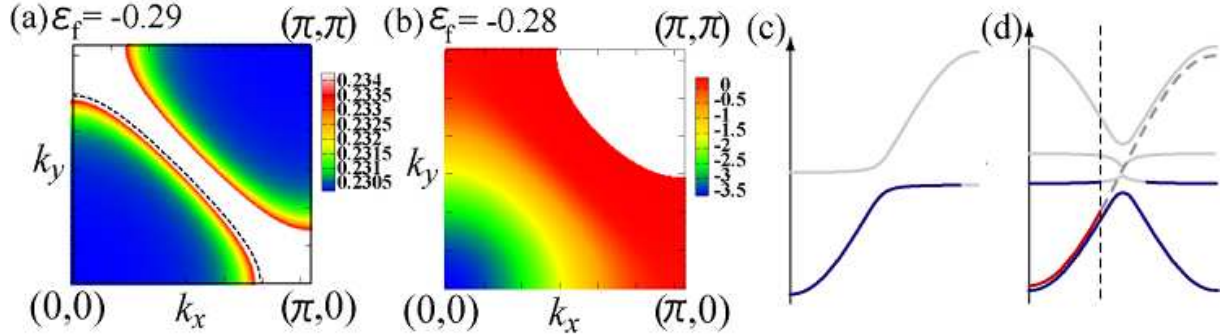


Figure 2. (color online) The contour plot of the energy band with \downarrow spin located at the Fermi level μ for $t = 1$, $V = 0.2$, $U = \infty$, $U_{fc} = 0.5$, and $n = 0.9$ with $h = 0.005$: (a) $\epsilon_f = -0.29$ and (b) $\epsilon_f = -0.28$. The $E_{\mathbf{k}\downarrow} > \mu$ parts are represented by white regions. In (a), the dashed line indicates the Fermi surface of the conduction band, $\epsilon_{\mathbf{k}}$ for $\bar{n}_c = 0.8$. Occupied (solid lines) and empty (gray lines) bands in the periodic Anderson model at $n = (\bar{n}_f + \bar{n}_c)/2 = 0.9$ are shown in paramagnetic phase (c) and in AF-ordered phase (d). In (d), gray dashed line indicates the energy band of the conduction band, $\epsilon_{\mathbf{k}}$ at $\bar{n}_c = 0.8$. Solid dashed line is a guide for the eyes indicating that the Fermi surface in AF-ordered phase with finite c-f hybridization coincides with the small Fermi surface where f electrons are completely localized.

These results are naturally understood if we draw the energy bands in the paramagnetic phase and the AF phase as in Figs. 2(c) and 2(d), respectively. In Fig. 2(c), the lower hybridized band of Hamiltonian (1) is occupied as illustrated by the solid line forming the “large” Fermi surface whose volume contains f electrons, i.e., $\bar{n}_f + \bar{n}_c$. On the other hand, the energy band of conduction electrons is illustrated in Fig. 2(d) by the gray dashed line whose occupied part for \bar{n}_c

is represented by the solid line, clearly indicating the “small” Fermi surface, in sharp contrast to Fig. 2(c). Once the AF order occurs, the lower and upper hybridized bands are folded as shown in Fig. 2(d). Since the lower-hybridized band in the magnetic Brillouin zone is fully occupied, the Fermi surface emerging at the folded lower-hybridized band shows the area occupied for the filling 0.8 among $n = (1 + 0.8)/2$, giving rise to the same Fermi surface of the conduction band at $\bar{n}_c = 0.8$. Namely, the “small” Fermi surface appears in the AF phase even though the c-f hybridization remains finite $\langle f_{\mathbf{k}\sigma}^\dagger c_{\mathbf{k}\sigma} \rangle \neq 0$. Thus, the mechanism of the coincidence of the Fermi surface in the AF phase and the dashed line shown in Fig. 2(a) is naturally understood.

We find that the total density of states $D(\mu) \equiv \sum_{\mathbf{k}\sigma} \delta(\mu - E_{\mathbf{k}\sigma})/(2N)$ at the Fermi level shows an enhancement toward $\varepsilon_f = \varepsilon_f^c$ as shown in Fig. 1(c). Here, μ is a chemical potential and $E_{\mathbf{k}\sigma}$ is the quasiparticle energy band with σ spin. The reason why such a mass enhancement occurs at the AF-paramagnetic boundary is explained as follows: In the AF phase, as ε_f increases, the gap between the folded lower-hybridized-band and the original lower-hybridized-band increases (see Fig. 2(d)). Then, the f-electron-dominant flat part of the folded band approaches the Fermi level, giving rise to the mass enhancement. In the paramagnetic phase, as ε_f decreases, \bar{n}_f increases to reach the $\bar{n}_f = 1$ state, i.e., to approach the Kondo regime. Hence, as ε_f approaches ε_f^c , mass enhancement occurs. Our result clearly shows that the mass enhancement is caused by the band effect including the local correlations of f electrons. This explains the experimental fact that the $\sqrt{A}/m^* = \text{const.}$ scaling holds under pressure from $P = 0$ to $P = P_c$ [5], where A is the coefficient of the T^2 term in the low-temperature resistivity at $H = 15$ T and m^* is a cyclotron mass of the β_2 branch of the cylindrical Fermi surface observed for $H = 12 \sim 17$ T in CeRhIn₅ [2]. For $P > P_c$, the dHvA signal of the β_2 branch was not detected [2], probably because of heavy effective mass larger than $m^* \approx 90m_0$ in CeCoIn₅. This is also consistent with our result shown in Fig. 1(c).

The Fermi wavenumber k_F defined by the crossing point of the line connecting $\mathbf{k} = (0, 0)$ and (π, π) , and the Fermi surface with minority spin at $h = 0.005$ exhibits the abrupt change at the AF-paramagnetic boundary as shown in the inset of Fig. 1(c). Thus, the drastic change of Fermi surfaces as well as the mass enhancement observed in the dHvA measurement [2] is naturally understood by our theory. We note that the density of states at $\varepsilon_f = -0.4$ is about 10 times larger than that of conduction electrons at $\bar{n}_c = 0.8$, $D_c(\mu) \equiv \sum_{\mathbf{k}} \delta(\mu - \varepsilon_{\mathbf{k}})/N = 0.092$, which is also consistent with the enhanced γ of CeRhIn₅ from that of LaRhIn₅ at $P = 0$ [2].

3. Summary

We have proposed a theory for resolving the outstanding puzzle on Fermi-surface change and transport anomalies in CeRhIn₅ in a unified way. The key mechanism has been shown to be the interplay of the AF order and Ce-valence fluctuations. Experimental tests to examine our proposal, in particular, direct observations of the Ce valence change under pressure and magnetic field near $P = P_c$ are greatly desired.

References

- [1] Hegger H *et al.*, 2000 *Phys. Rev. Lett.* **8** 4986.
- [2] Shishido H *et al.*, 2005 *J. Phys. Soc. Japan* **74** 1103.
- [3] Park T *et al.*, 2006 *Nature* **440** 65.
- [4] Park T *et al.*, 2008 *Nature* **456** 366.
- [5] Knebel G, Aoki D, Brison J P, and Flouquet J, 2008 *J. Phys. Soc. Japan* **77** 114704.
- [6] Jaccard D, Wilhelm D H, Alami-Yadri K, and Vargoz E, 1999 *Physica B* **259-261** 1.
- [7] Holmes A T, Jaccard D, and Miyake K, 2004 *Phys. Rev. B* **69** 024508.
- [8] Yuan H Q, Grosche F M, Deppe M, Geibel C, Sporn G, and Steglich F, 2003 *Science* **302** 2104.
- [9] Fujiwara K *et al.*, 2008 *J. Phys. Soc. Japan* **77** 123711.
- [10] Miyake K and Maebashi H, 2001 *J. Phys. Soc. Japan* **71** 1007.
- [11] Watanabe S and Miyake K, 2010 *J. Phys. Soc. Japan* **79** 033706.
- [12] Kotliar G and Ruckenstein A E, 1996 *Phys. Rev. Lett.* **57** 1362.